The Ignitor Diagnostic Systems

From "Ignitor Experiment: General Report, Part I, Physics Guidelines and Design criteria"

Contributing Authors: R. Bartiromo, P. Batistoni, E. Bittoni, F. Bombarda, G. Bonizzoni, P. Buratti, S. Coda, B. Coppi, P. Detragiache, C. Ferro, G. Gorini, M. Haegi, J. Källne, H. Kroegler, E. Mazzucato, M. Nassi, S. Rollet, O. Tudisco, M. Zerbini, M. Zucchetti.

1. General Considerations

The scientific objectives of Ignitor, centered on the study of fusion burning plasmas, lead to a choice of diagnostic systems that give priority to those objectives and have a special set of characteristics [1]. These systems have to withstand large fluxes of neutrons and γ-rays which are produced in the surrounding materials. This hostile radiation environment introduces new problems, like radiation induced background and permanent damage to components such as detectors and electronics. The selection of diagnostics tools for an ignition experiment should therefore be based on a set of strict rules. All diagnostics must have a high degree of reliability; a straight line of sight plasma-detector should be avoided as much as possible, and instruments must allow the placement of the detection section at a safe distance from the plasma where it can be properly shielded. A set of important diagnostic systems satisfying these criteria are discussed in sections 3-5. The large fluxes of fusion neutrons produced by Ignitor allow an extensive use of neutron diagnostics that are described in section 5. In fact, a precise determination of total fusion power generated and thus the crucial demonstration of ignition can be obtained by neutron measurements. Useful information to characterise the plasma is obtained by measuring the time dependence and spatial distribution of the neutron flux produced during the discharge.

2. Electromagnetic Diagnostics (F. Alladio)

This set of diagnostics is presently being re-designed to meet the latest specifications of the vacuum vessel.

3. Plasma Diagnostics

Electron Temperature

In the following, the characteristics of two methods for the measurement of the electron temperature in the Ignitor experiment will be described: Electron Cyclotron Emission (ECE) and Thomson Scattering of laser light.

A. Electron Cyclotron Emission (P. Buratti and M. Zerbini)

Accurate measurements of electron temperature profiles with good spatial and temporal resolution can be obtained from the spectral analysis of Electron Cyclotron Emission (ECE) at optically thick harmonics. A high optical thickness is obtained for very wide ranges of plasma parameters at the fundamental frequency in the ordinary polarization and at the second harmonic in the extraordinary polarization [2]. Various kinds of ECE diagnostics are widely used for transport analysis, for heat pulse propagation, for diagnosing MHD phenomena, and in some cases for feedback control.

In low aspect ratio toroidal devices the spatial extent of temperature profiles that can be obtained from ECE is conditioned by the overlap between different harmonics. For full-bore discharges with R_0=1.32 m and a=0.47 m, the following limits arise on the accessible major radius R:

fundamental harmonic: $R_0 - 0.42 \leq R \leq R_0 + a$

second harmonic: $R_0 - 0.12 \leq R \leq R_0 + 0.37$

The accessibility of the resonance layers is also conditioned by the existence of cutoff layers: the fundamental harmonic is not accessible in the extraordinary mode, while the condition for the o-mode is $n_e < 0.1\ B^2$, where n_e is expressed in units of 10^{20} m^{-3} and B in T. For some

scenarios (e.g. for $n_e=8\times10^{20}$ m^{-3} and B=10 T) the condition is only marginally fulfilled, and, although the cutoff is absent, ECE is affected by strong refraction and by reduction of optical thickness. For the second harmonic, x-mode, the condition is $n_e < 0.2\ B^2$, and finite density effects are negligible. As a conclusion, the combination of low aspect ratio and high density implies that two harmonics must be used for a full measurement of temperature profiles in all regimes, namely the fundamental in the o-mode and the second harmonic in the x-mode.

The radiation temperature is in equilibrium with the electron temperature (blackbody emission) provided that the optical thickness $\tau \gg 1$; in addition, high τ means a low effective resonance width, thus preventing the degradation of spatial resolution at high temperatures. For the fundamental harmonic in the o-mode and density well below the critical value, we have: $\tau_1=18.5\ n_e\ T_e\ R / B$, with R in meters, T_e in keV, n_e and B as before. For the second harmonic, x-mode: $\tau_2=2\times\tau_1$. For both harmonics the optical thickness is high for a very wide range of parameters.

The line of sight is usually directed along a major radius on the equatorial plane; this choice optimises the spatial resolution and allows to select the desired polarisation mode simply by a linear polariser. The fact that the radiation temperature in a spectral element equals the electron temperature in a well-defined plasma volume element implies that a full 2-D mapping of the electron temperature could be obtained by adding different lines of sight. It has been verified at JET that such a reconstruction does not add significant information to the one obtainable from a single line with the assumption that flux surfaces are isothermal, but using at least one additional line the accuracy of flux surfaces reconstruction can be verified. Additional lines of sight could also be required to resolve the mode numbers of MHD oscillations.

The electron cyclotron frequency, in GHz, is given by $\nu_1 = 28\ B$, so that the fundamental range is $114 \le \nu_1 \le 568$ GHz for B_0=5.5-13 T, and the second harmonic range is $228 \le \nu_2 \le 1136$ GHz. Such spectral ranges could be analysed by a Michelson interferometer and by a multiple grating polychromator, with the exception of the fundamental range at the lowest field, for which the signal-to-noise in the polychromator could be low. In the latter range a heterodine radiometer could be used.

The spatial resolution along the line of sight depends on the spectral resolution; in fact, radial profiles are obtained from spectral ones owing to the spatial variation of the cyclotron resonance frequency. The light collection system determines the spatial resolution in the direction perpendicular to the lines of sight; in addition, the stability of the alignment is critical for the reliability of ECE diagnostics. There is no simple optical or waveguide system that can provide both good spatial resolution and stability on machines with a relatively long distance between the plasma and the vacuum window. A combined scheme suitable to fulfill both requirements has been developed for the FTU tokamak [3] and can be applied to Ignitor to obtain a spatial resolution of 3 cm in all directions and a light collection suitable for detector-limited performance. The FTU scheme includes a lightpipe in the torus vacuum and an external optical system which determines both spatial resolution and polarization. Radiation selected by the optical system is carried to the spectrometers by a long pipeline. Since the vacuum lightpipe is not accessible, an identical one which can be presented to the optical system by turning a mirror is used to calibrate the ECE diagnostics on FTU. A similar calibration scheme can be devised for Ignitor as well, in alternative to the development of a calibration source which can operate in the torus vacuum.

The time resolution depends on the employed spectroscopic method. For polychromators and multichannel radiometers a resolution of a few microseconds can be obtained (the limit in this case is the signal-to-noise ratio rather than the speed of the instrument). For multiplexing instruments such as the fast-scanning Michelson interferometer, the time resolution is determined by the scan time; by using rotating scanning devices a scan time of 5 ms can be easily obtained [4, 5].

Systematic errors on temperature values depend on the accuracy of the absolute calibration of the Michelson interferometer; the calibration technique used for FTU yielded an accuracy of 5% in best conditions (i.e. at high field). The accuracy on the determination of the correspondence between spatial position and spectral frequency depends on the knowledge of the magnetic field profile; this can be a serious problem in the presence of large poloidal and toroidal magnetic fields generated by currents flowing in the plasma, because the error on position is proportional to the major radius, so that a 5% error on B gives an error of 8 cm on position.

The data analysis for the Michelson interferometer requires quite a complex software, but the application of the Fortran package developed for FTU would be straightforward for off-line data analysis and display. At present, plasma magnetic fields are calculated recursively from measured temperature profiles; an improvement could be obtained using data directly from magnetic measurements. If real-time data were required for plasma control, proper hardware and software tools should be implemented. Data analysis for the polychromator is simpler, even for the case of feedback control.

Proposed lay-out. A system of ECE diagnostics which exploits the diagnostic potential with minimum complexity should include the following subsystems:

1) An equatorial light collection line followed by two transmission lines (one for the o-mode and the other for the x-mode) each connected to a Michelson interferometer. This subsystem should be absolutely calibrated. This subsystem should be the main one for profile measurement.
2) A subsystem similar to 1, but with its line of sight displaced vertically, to be used to check the plasma shape.
3) An equatorial o-mode line connected to a polychromator, to be used for the analysis of MHD activity.
4) A subsystem similar to 3, at a different toroidal location.
5) A subsystem similar to 3, with a different view in the poloidal plane; this could share the access of subsystem 2.

Spectral analysis for subsystems 1 and 2 could be performed by a compact four-channel Michelson interferometer [6]. For low-field operations, the polychromators should be substituted by multichannel radiometers.

B. Thomson Scattering (E. Giovannozzi)

Owing to the fundamental importance of the electron temperature, another independent measurement of this quantity is necessary. This can be obtained with Thomson scattering of laser light. The Ignitor design allows the injection along a vertical direction of a low divergence (≤ 0.3 mrad) laser beam. The scattered light can be collected through a window on the mid plane,

and brought with a fiber-optic bundle to a remote location where its spectrum is analysed and measured with an array of intensified charge couple devices [7]. This technique provides the vertical profile at one time in a discharge of both the electron temperature and density. The temperature profile obtained from Thomson Scattering can also be used for checking the calibration of the ECE polychromator.

Ion Temperature (F. Bombarda)

The value of the ion temperature can be obtained from neutron measurements (as described in a separate paragraph) and from the Doppler broadening of highly ionised impurity lines. Two types of instruments can be used for Doppler broadening: vacuum ultraviolet monochromators [8] and X-ray crystal spectrometers [9]. The latter is probably the only X-ray technique which can survive in an ignition experiment, since the X-ray diffracting crystal provides a mean of removing the detector from the direct neutron beam produced by the plasma. Both of these techniques can also provide information on impurity concentrations and, in combination with bolometric measurements [10], on radiation losses. High resolution curved crystal spectrometers have become a fairly standard diagnostics for plasmas with temperature above ~1 keV. A convenient range of observation is between 1.5 and 4 Å, where the resonance spectra of H-like and He-like elements from argon to nickel are located, but also lines from $Mo^{30+,31+,32+}$. In Ignitor, some metal impurities can be expected from the molybdenum first wall; otherwise the spectroscopy measurement for the ion temperature should rely upon impurity injection. Trace quantities (10^{-3}-$10^{-4} \times n_e$) are usually adequate for this kind of measurements, given the high throughput of the curved crystal spectrometers. Argon has proven to be a very convenient element to use for this purpose, but it will not be suitable for the high temperatures envisaged. The next gaseous element would be krypton, recently observed in TFTR [11]. Transition metals from titanium to nickel or copper are more suitable, and they could be injected in a steady way by letting the surface of a metallic probe to be eroded by the plasma itself, as it was done on FTU with titanium, or by means of more sophisticated evaporation techniques. Laser blow-off produces a very transient signal, which can be useful for the determination of the particle diffusion coefficients but not for following the T_i evolution during the discharge.

A spectrometer in the Johann configuration is a very suitable instrument in a high background radiation environment, because it allows the positioning of the crystal at a considerable distance from the plasma (the throughput scales only as the inverse of the distance, rather than the inverse square) and the detector can easily be shielded. Focal lengths of the order of 20 m have been achieved, though in the case of Ignitor half that distance is probably needed. Bragg angles around 50° or more are typical for this type of instruments. Depending on the torus hall size, it may be more convenient to place the crystal, with the detection arm and detector, outside the biological wall, in an adjacent room, which, however, will have to be properly screened. Alternatively, the whole instrument could be located inside the torus hall, if adequate shielding around the detector can be installed. The input arm, connecting the machine to the crystal, is fixed, whereas the output arm should have the possibility of pivoting to some extent around the crystal, to allow the proper choice of spectral range to be observed according to plasma conditions and available impurities. In present experiments, the measurements of the ion temperature spatial distribution is more difficult than that of the electron temperature profile. This is likely not to be a serious problem for Ignitor because, owing to the very high plasma density expected in this experiment, the values of the two temperatures should be very similar. In its simplest form, a single quartz crystal and a Multiwire Proportional Chamber (MWPC) can provide a measurement of the ion temperature along a single line of sight, with a spatial resolution that can be determined either by the dimension of the emitting region in the plasma or by the relative sizes of the crystal and the detector, in both cases of the order of 20 cm. Two-dimensional MWPCs allow to achieve spatial resolution in the vertical plane of the order of 1 cm, by inserting a horizontal slit between the crystal and the detector [12]. No movement of the crystal or of the detector is required, and the spectra for all the chords are collected simultaneously. With the compact design of the Ignitor machine, it is difficult to observe a larger fraction of the poloidal plane than the simple height of the horizontal port. On the other hand, the dimensions of neither the detector or the crystal can be extended indefinitely. As a matter of fact, the imaging of 800 mm of plasma on a 200 mm detector would require a 300 mm high crystal, which is not available, and a stack of crystals is necessary. This solution presents the advantage of multiple, relatively small diameter input arms and small beryllium windows. An alternative scheme uses a single crystal and 3 detectors. Typical time resolution with this kind of

instruments are of the order of 10 to 100 ms; choosing the proper impurity for the given plasma temperature can ensure an adequate photon flux, and the aperture of the slit should also be adjustable to allow greater flexibility in counting rate.

As mentioned before, the geometry of the curved crystal spectrometer removes the detector from the direct line-of sight of the plasma, considerably reducing the problems connected to the neutron and γ background. A certain amount of scattering, however, should be expected, and that would result in background noise at the detector, mainly due to the radiation induced in its mechanical supporting structure. Electronic discrimination of the background radiation induced signals is possible, should the noise level be too high [13].

The analysis of other spectral features allows the measurement of the electron temperature, for example, from the line intensity ratio of a dielectronic satellite to the collisionally excited resonance line. Absolute line brightness can also be used to measure the impurity density. The instrument throughput is not actually measured, but it can be calculated from crystal reflectivity, overall transmission and geometry, to a reasonable level of accuracy. In order to extend the radial range for the ion temperature profile, a grazing incidence, XUV spectrometer can be used to measure the Doppler broadening of lighter impurities lines, such as C, O, He, in the spectral range from 100 to 350 Å [14]. In this case the spatial resolution is given by the localization of the emitting region, as determined either from the observation of a survey spectrometer with spatial resolution, or from the calculations of an impurity transport code.

Plasma Density (O. Tudisco)

Density is a crucial parameter that is needed not only for physics evaluation but also for machine operation. In the following, three methods for the measurement of the plasma density in Ignitor will be described: a Two Colour CO_2 Interferometer, a densitometer based on Faraday rotation and a technique based on microwave reflectrometry.

A. Two Colour CO_2 Interferometer.

Density measurements by Two Colour interferometers (TCI) with CO_2 laser (10.6 μm) have been made on several machines (RFX [15], DIII-D, and Alcator C-Mod [16]). This technique avoids the expensive anti-vibrating structure that is necessary with single colour

interferometers. The phase error introduced by vibrations is compensated through the use of a second colour interferometer that shares the same optical components. The choice of a 3.39 μm of a HeNe laser as second colour is more convenient than a visible line, because vibrations result in lower frequencies components on the output signal.

Let us call V the characteristic vibration velocity of the optical elements of the interferometer; the characteristic velocity shift generated is $f \cong v/\lambda$, where λ is the laser wavelength. If B is the bandwidth of the electronics, then the maximum velocity that can be supported is of the order of λB. For λ = 3.39 μm and B = ± 1 MHz, we obtain $V_{max} \approx 3.4$ m/s. Higher velocities can be accepted by increasing the bandwidth.

The Ignitor tokamak, being a compact high field device, has narrow vertical ports, looking at the plasma through the center and out to about half the minor radius. Excluding the possibility of placing retroflectors on the inner side of the vacuum vessel, because too close to the plasma, a horizontal port could be used to increase the number of chords for a better mapping of the density profile. In Fig. 2 a sketch of one of the Ignitor poloidal sections is presented, with four tentative chords. One of the lower vertical penetrations centered on axis is used to launch four beams, with retroflectors placed in the upper vertical port and on the upper wall of the horizontal port. A more complete covering of the plasma poloidal section can be obtained by making use of another port, at a different toroidal location, with an outer vertical view of the plasma. The possibility of using a set of horizontal chords laying on the equatorial plane has also been analyzed without success. Due to the strong dependence of the plasma delay on the polarization of the beam, on the angle between the beam direction and the magnetic field, and on the strength of the magnetic field itself, its interpretation becomes cumbersome.

B. Densitometer by Faraday Rotation.

The possibility of measuring the plasma density of large tokamak by equatorial Faraday rotation has been suggested by other authors [17]. As suggested in ref. [17] the main advantages of using Faraday rotation with respect to interferometry are:

1) the rotation is always less than one fringe;

2) only one horizontal window is used instead of 2 large vertical windows (usually difficult to have in a compact machine as Ignitor);
3) the rotation angle is insensitive to the vibrations and the optics can be anchored to the vacuum vessel directly. On the other hand, the toroidal magnetic field must be known exactly and interpretation problems can arise from ripple and diamagnetic fields.

This measure is based on the following technique**.** A linear polarised laser beam is launched into the plasma along the equatorial plane tangentially to the toroidal magnetic field. The Faraday rotation of the polarisation depends on the electron plasma density and from the component of toroidal magnetic field along the beam trajectory. This rotation is given [17]:

$$\phi = (1/2c)(\lambda/2\pi c)^2 \int dl \cos\theta \ \omega_{pe}^2 \ \Omega_{ce} \ =$$

$$= g \, B_t \, R_t \int dl \, n_e \, (R) \, R_t \ / R^2$$

where c is the light velocity, λ is the radiation wavelength, θ is the angle between the toroidal magnetic field and the light path *l*, Ω_{ce} and ω_{pe} are the cyclotron and plasma angular frequencies, R_t is the major radius of the point of tangency of the beam to the magnetic field and B_t is its value at that point. The constant $g = 5.9 \times 10^{-23}$ m^2/T for $\lambda = 10.6$ μm, single pass.

The contribution of the poloidal field to the Faraday rotation is negligible as it is always perpendicular to plane of propagation of the beam. It is interesting to note that this contribution remains negligible even if the plane of propagation is different from the equatorial plane, provided that they keep to be parallel. In fact, the contribution before the tangency point is equal and of opposite sign to the contribution after that point, as the plasma is axisymmetric. If a flat density profile is assumed, the rotation angle is given by $f = g \, n_e B_t R_t \psi$ where ψ is the toroidal angle subtended by the beam, and for Ignitor parameters (R_0=1.32 m, *a* = 0.47 m, B_0 = 13 T, $n_e = 6 \times 10^{20}$ m^{-3}) it yields, for a double pass, a maximum rotation of 2.6 rad, for the chord with $R_t = R_0$-*a*. When a parabolic profile of density is assumed, the maximum rotation is obtained close to $R_t = R_0 - a/2$ and is about 3 rad for a double pass and a peak density $n_0 = 1 \times 10^{21}$ m^{-3}. Both these values are well below one fringe so that at any time the data do not depend on the history of the measurement.

Considering the actual design of Ignitor horizontal ports, it is possible to build an horizontal polarimeter with 12 channels, using a CO_2 laser source. The 12 channels consist of

two groups of 6 channels that lay on two different planes, the equatorial (Z=0) and at half of the vertical size of the vacuum vessel (Z=*b*/2). An horizontal port must be employed to launch the beams, while retroreflectors can be held using three other ports at the angular distance of 60°, 90° and 120°. Two retroreflectors can be put in each port, in the equatorial plane, using the pocket present at the end of the port. In this way the retroreflectors can be kept angularly distant and held far enough from the plasma (about 10 cm). The radii of the beam tangency points relative to the six chords laying on the equatorial plane, could be made close to the following values: -*a*, -0.73 *a*, -0.20 *a*, 0.08 *a*, 0.54 *a* and 0.73 *a*.

The other 6 channels could be made reproducing the same system of the equatorial plane just shifting everything vertically to the top of the port. This plane has a height of 0.45 *b*. All the considerations made before are also valid for this plane, so that the six retroreflectors could be placed above the ones of the midplane. Even if the paths of these channels are parallel to those in the midplane, they never cross the plasma core and the contribution to the polarisation rotation will be different from the corresponding beam in the midplane. They will be useful for the determination of the profile in the outer region of the plasma.

The inversion of the data, relative to the midplane beams, can be easily performed if the toroidal magnetic field is assumed to be $B = B_0R_0/R$, without ripple and paramagnetic effects, and no refraction occurs on the beams. If these effects cannot be neglected, the exact toroidal magnetic field should be imported from other diagnostic (as equilibrium reconstruction) or should be computed by an iterating technique using the pressure profile. The analysis of the other six channels requires, in any case, the knowledge of the equilibrium reconstruction and the assumption that n_e is a flux function.

C. Reflectometry

Microwave reflectometry is a new promising technique for the measurement of electron density profiles with minimum requirements of diagnostic access. Density profiles are reconstructed from measurements of round trip group delay vs. frequency for electromagnetic waves reflected at a cutoff layer, so that a single line of sight is required. On existing toroidal devices both the plasma frequency cutoff ($f_{pe}=90n_e^{1/2}$, with f_{pe} in GHz and n_e in $10^{20}m^{-3}$) for the

ordinary polarization and the upper cutoff $\{f_R=[f_{pe}^2+(0.5f_{ce})^2]^{1/2}+0.5f_{ce}$, with $f_{ce}=28B\}$ for the extraordinary one have ben used. When the f_R cutoff is used the entire density profile is accessible because the cutoff frequency is a unique function of the major radius, but the required frequencies would be very high for Ignitor (up to 570 GHz). Using the f_{pe} cutoff, only part of the profile is accessible. In fact, the cutoff frequency is a decreasing function of the major radius only on the low field side. Furthermore, the probing frequency must be lower than the minimum cyclotron resonance frequency, i.e. 270 GHz at B=13 T; the corresponding maximum critical density is 9×10^{20} m^{-3}. A third possibility is to use the lower cutoff for the extraordinary mode ($f_L=\{f_{pe}^2+(0.5f_{ce})^2\}^{1/2}-0.5f_{ce}$); in this case the required frequencies are much lower, as the maximum foreseen density, i.e. 10^{21} m^{-3}, corresponds to a cutoff frequency of 156 GHz at B=13 T and of 178 GHz at B=10 T. The f_L cutoff has never been used before since it is not convenient for low field devices. It is however attractive for high field applications, as the use of probing frequencies below 200 GHz greatly reduces the degree of the technical difficulty. Measurements on the f_L cutoff are in progress on the FTU tokamak.

The main problem experienced in the measurement of density profiles by reflectometry arises from density fluctuations which distort the reflecting layer, giving rise to strong amplitude and phase modulation of the reflected beam. Several techniques have been developed in order to minimize the effects of fluctuations:

1) extremely fast scanning FM reflectometry, in which the measurement time is small compared to the fluctuation period;
2) pulse radar reflectometry, in which time-domain measurements are performed;
3) AM reflectometry, in which the phase difference between two probing waves with slightly different frequencies is measured. The evaluation of these techniques is in progress on several tokamaks and stellarators. The AM technique seems particularly promising for applications in which high frequencies and large distances between the plasma and the instruments are required.

Spectroscopy (F. Bombarda)

The observation of radiation emitted by H, D, O, C, and all the elements of the plasma facing components, in the visible to the VUV spectral range, has always been an essential tool for

understanding plasma behaviour in tokamaks. Visible spectroscopy, in particular, has been greatly revived in recent experiments, due to the increased interest on edge phenomena, where most of the visible light is emitted, but also for the possibility, offered by the use of optical fibers, of removing the sensitive parts of the diagnostics to a sufficiently remote location, where neutron and γ background can be avoided. For these reasons, a comprehensive set of spectroscopic instruments should be implemented on Ignitor, making extensive use of fiberoptic bundles to image the plasma at a distant location and beam splitters to share it between different instruments. A full image of the plasma cross section can be obtained with 3 or 4 views from the top, bottom and side of the machine, possibly placing the head of the fiber bundles behind a window on re-entrant tubes. The images transmitted by each bundle can then be beam-splitted and viewed in one or two colors with interference filters and finally focused on diode arrays. The purpose of having a large number of chords with suitable spatial resolution is to be able to provide absolute line brightness that can be inverted to give local emissivity in a poloidally asymmetrical geometry. The time evolution of H_α, D_α, and selected lines of C (for example, at λ = 465 nm for C^{+2}) provides informations about the plasma edge conditions, fueling and impurity sources. One high resolution (R>4000), broad range visible spectrometer can be employed to measure both the line widths and the intensity ratios of individual lines. Czerny-Turner instruments with 1 or 2 m radii are currently used on many tokamaks. Doppler, Stark and Zeeman effects can all be expected to contribute to line shapes and splittings, and a number of informations can be gathered from their observation: ion temperatures, electric and magnetic field values, rotation velocities, edge electron densities. Finally, a survey spectrometer in the VUV range, with interchangeable gratings should also be included, since the general monitoring of all impurities is important throughout the life of the experiment. McPherson spectrometers are also commonly used for this purpose, and their absolute intensity calibrations have become more reliable. However, this type of instruments, like all the others directly connected to the tokamak vacuum, are not easily made radiation hard.

Radiated Power (H. Kroegler)

Time and space resolved measurements of the total plasma radiation can be done by means of multichannel arrangement of bolometers. The bolometers have to determine quantitatively the total emission in the spectral range from 0.1 to 200 nm which corresponds to an electron temperature of about 5 eV to 10 keV. Neutral particles are measured but charged particles, neutrons, γ radiation and hard X-rays do not contribute to the measured signal. The time resolution is determined by the electronic circuit and may be selected from 1 ms to 100 ms. Space resolution in the poloidal plasma cross-section has to be sufficient to evidence contours of emissivity; 36 viewing horizontal chords should be sufficient to meet this requirement. Since the Ignitor plasma has a non-circular shape and the vertical ports are too narrow to apply additional viewing chords, the reconstruction of the distribution of the radiation emission can be done by an algorithm assuming constant emissivity on flux surfaces [18,19].

The sensor heads are required to have a flat spectral response from about 1 Å to 2000 Å, where the major part of the power losses lies; it should be possible to perform the bolometer calibration in-situ and the calibration data should not drift with time. Furthermore, the bolometer sensors have to work in-vessel under extreme environmental conditions: baking-out temperature 600 K, ultra-high vacuum, neutron and γ radiation during D-T operations, magnetic fields up to 13 T.

The temperature rise ΔT of the bolometer absorber layer due to the uniformly incident radiation power P_{in} is governed by the differential equation

$$P_{in} = C\left[\frac{d}{dt}\Delta T + \frac{\Delta T}{\tau_c} \right]$$

where C is the thermal capacity of the absorber and τ_c is the cooling time constant. As the absorber area and the thickness are small, a homogeneous and instantaneous (<100 μs) temperature can be assumed. The differential equation states that the measure of the time dependence of T permits a determination of the radiation emitted from the plasma as a function of time. The signal of one bolometer-channel is proportional to the line integral of the emissivity along the measuring chord through the poloidal plane. Summing up the intensities of all chords gives approximately the total power losses. The radial profile of the local radiation density is calculated numerically from the cord intensities by applying an inversion method. A good value

of the total power losses is given by integrating the emission profile over the entire poloidal plasma section.

A so called metal-resistor bolometer sensor is proposed for performing radiation measurements in Ignitor. It is a small-sized four-bolometer module with four active and four reference bolometers shielded against radiation. It offers the advantages of meeting Ignitor requirements and of having already been tested in ASDEX, JET, TORE SUPRA and FTU. This type of bolometer has proven to be rugged and, due to the reference compensation, relatively immune to electrical noise and thermal drift.

A rectangular (1.3 x 3.8 mm) 4 μm thick gold foil absorbs almost totally the radiation from about 10 Å to 2000 Å; the subsequent temperature rise of the foil causes an increase of the 1 kW gold resistor which is separated from the gold absorber by a 7.5 μm kapton foil. The small temperature coefficient of the gold resistor (0.0026 $°C^{-1}$) is compensated by applying a bridge circuit of two active and two reference resistors. Metal-resistor bolometers have shown to be very reliable, stable and free of radiation-damage, whereas other existing types of bolometers are extremely sensitive to radiation damage by neutron and γ radiation causing lattice defects as well as ionization in the resistor layer.

To extend the light absorption of the gold foil to the infrared it could be possible to blacken the gold absorber surface. By increasing the thickness of the gold absorber foil to about 15 mm, the absorbed spectrum range can be enlarged down to 1 Å.

A very simple method to calibrate a metal-resistor bolometer is to apply a square wave excitation current to the bolometer-bridge to transfer an ohmic heating power of a known quantity to the bolometer foil. This approach gives quiet good results in comparison to a second method based on measuring the response to a light beam of calibrated intensity and has the advantage that it can be applied for all bolometers of an array in-situ.

If a uniform distribution of the radiation and of the neutral particle emission is assumed and the plasma is considered as an isotropic radiation source, then a very crude signal estimate can be given. The D-T scenario with maximum parameter regime has a total radiated power of about 10 MW uniform distributed to the whole plasma surface of 10 m^2 which gives a surface radiation density of 16 W/cm^2sr. The layout of the horizontal ports suggests a acceptance solid-angle Ω = 0.5 msr, resulting in a total power deposition on the bolometer absorber foil of about 4

mW. This gives, applying the FTU calibration data, a signal of about $\Delta V = 40$ mV. In order to be able to measure small variations of the emitted power, a special electronic chain has been developed and is available commercially. The bolometer-bridge is supplied by an AC (10 kHz - 50 kHz) voltage. The small signal requirements and the distance between the bolometer and the data-aquisition equipment are covered by a pre-amplifier. Due to the tolerances in its resistive elements, the bridge has an inherent AC offset voltage which is added to the signal voltage in a summing amplifier whose output is adjusted to a low, well-defined amplitude. The main amplifier has two variable-gain stages and feds the signal to a synchronised rectifier and to a low-pass filter. This filter is necessary in order to suppress the carrier frequency and to restore the modulation signal, which represents the desired information. The bolometer pinhole camera is connected to the vacuum chamber and electrically insulated by optocouplers from the electronic system. This prevents electric loops and flashover between the bolometer and the vacuum vessel. The amplifier-gain and the filter cut-off frequency settings are established by a GPIB communication link.

In connection with the D-T scenarios two questions arise: is the bolometer insensitive enough to radiation damage and what radiation shielding procedures have to be adopted for the electronics? The neutron fluxes cause activation of the machine and all diagnostics attached to it. In the event of damage, the replacement and repair has to be done by remote handling. Fast neutrons can cause severe radiation damage in many materials and electronic components. γ radiation can cause radiation damage just like neutrons but not activation. The radiation damage in kapton has been studied in detail [20]. The main types of radiation damage are ionisation of the polimeric material, excitation or even dissociation of molecules, and formation of free radicals resulting in degradation of the material characteristics. Kapton can be used up to radiation doses of 5×10^9 rad without losing its insulation properties [21]. The effect of tritium is that it can replace normal hydrogen in chemical compounds by isotopic exchange reactions and has to be taken into account with respect to the kapton insulation of the bolometer, but no experimental data about kapton have been published. Concerning the electronics exposed to neutron and γ-radiation similar considerations have to be done. Semiconductors are much more sensitive to radiation damage than metals and therefore the whole electronic equipment has to be

shielded by thick boronated concrete walls. In any case there should be an easy access to facilitate the replacement.

In conclusion, a well known and tested diagnostic tool is proposed to perform a local energy balance and investigate plasma-wall interactions. A bolometer pin-hole camera based on metal-resistor sensors seems to be the most suitable. The bolometer camera should be attached to a port far away from the cold gas inlet and from all applied additional heating systems because in their neighbourhood the bolometer signal can be falsified. Further investigations and tests should be done to clear up the influence of tritium on the kapton insulator.

4. α-Particle Effects (M. Haegi)

Unlike presently operating experiments, Ignitor is designed to produce massive α-particle heating. Therefore this is expected to become well evident through the energy balance and the peak plasma pressures that can be achieved. We note that when the plasma current is in the range $10 \leq I_p \leq 12$ MA the α-particle orbits are estimated to be well confined in the center of the plasma column [22]. For all these reasons we have given a definite priority to the study and planning of neutron diagnostics, while following closely the performance of the direct α-particle diagnostic systems that have been developed for the D-T experiments by the JET and the TFTR machines. In addition, proper attention has been paid to the proposal of different diagnostic techniques [23] that are particularly suitable for the plasma parameters that Ignitor can be expected to produce.

5. Neutron Diagnostics (P. Batistoni, G. Gorini, J. Källne)

In the investigation of Ignitor physics, an important role is played by neutron diagnostics which should provide information on the plasma parameters and on the plasma response to external controls, such as heating power, fuelling, etc. When significant fusion rates are achieved, neutron diagnostics could give some insight into the α-particle behaviour (confinement, thermalisation rate) and their effects on the background plasma (heating rate, instabilities). Apart from information on ion density and temperature, the high neutron flux levels

expected for Ignitor will allow measurements with good space, time and energy resolution, providing information on plasma profiles and on the ion velocity distribution function. Neutron diagnostics can also provide useful information on α-particle issues, like the total a power $P_\alpha(t)$ and its spatial distribution.

There are several technical reasons for developing neutron diagnostics for Ignitor in addition to other diagnostics:

1) the high radiation level accompanying high fusion power is of concern to diagnostics. For neutron diagnostics this is ameliorated by the fact that the signal to background ratio is not deteriorated and the intense neutron signal would improve the counting statistics;
2) the interface between the diagnostics and the tokamak is generally a difficult problem curtailing the information output. Neutron diagnostics have fewer interface problems than most other installations;
3) finally, access to the plasma (port space) is limited with a high value of the benefit/cost ratio.

The diagnostic capabilities of neutron measurements in Ignitor have been investigated in a recent study [24], by means of a calculation model of the device. The analysis was based on a calculation model of the Ignitor device using the 3-D Monte Carlo code MCNP [25], used to anticipate the neutron flux levels and the related energy spectra in different parts of the device, which are of interest for the diagnostic project and exploitation. In this model all the main device components are represented (plasma chamber, TF coils, PF coils, C-clamp, central post, press, ports etc.). The model has been used to simulate a 14 MeV neutron source, with a gaussian spectrum with a FWHM of 560 keV corresponding to T = 10 keV. The Ignitor plasma was represented by an extended neutron source with equi-emissivity surfaces having D-shaped cross section with the same ellipticity and triangularity as the plasma chamber. The source spatial distribution was given by a generalised parabola with exponent equal to 7. The numerical results have been used for the design of a complete set of neutron diagnostics including:

1) the counters and the activation technique to measure the total neutron yield;
2) the multicollimator array to measure the radial distribution of the neutron emissivity;
3) the high resolution spectrometers to measure the neutron energy distribution.

Total Neutron Yield Measurements

The planned plasma scenarios for the Ignitor D-T phase scan from low to extreme parameter regimes, where the neutron production rate can vary by more than two orders of magnitude, from about $Y_n(t) \approx 10^{17}$ to about 10^{20} n/s. Large variations are also expected in single discharges: for example, the rise phase of the plasma current, lasting 4 seconds, is characterised by a strong rate of ohmic heating up to relatively high temperatures. The neutron production rates vary by several orders of magnitude in this phase, from $Y_n(t) \approx 10^{15}$ to about 10^{20} n/s in the extreme regime. In this regime, the current flat top phase lasts 4 seconds during which the neutron production rate may well exceed the expected value of Y_n at ignition ($Y_n \approx 3 \times 10^{19}$ n/s).

The primary piece of information obtainable by the measurement of $Y_n(t)$ is either the ion temperature or the ion density time variation, provided that the other one is known independently. The limited use of auxiliary heating (which can cause strong supra thermal neutron production) would mean prevailing thermal plasma conditions in Ignitor, favourable to the interpretation of neutron measurements. The other important aspect is that, in ignited plasmas, the measurement of $Y_n(t)$ is essential for monitoring the total fusion power $P_\alpha(t)$ carried by the α-particles which are produced concurrently with the 14 MeV neutrons. Hence the quality of the total neutron yield measuring system is mainly defined by two aspects, i.e., the achievable time resolution and the absolute calibration of detectors.

In present fusion devices characterised by $Y_n(t) \geq 10^{13}$ n/s, like for example JET, TFTR and also FTU, the neutron yield measuring systems involve the use of fission chambers. For instance, ^{235}U fission chambers are sensitive to thermal neutrons (since the fission cross section for ^{235}U is highest at neutron thermal energies) and are embedded in suitable moderators. In the presence of very high flux levels, fission chambers sensitive to fast neutrons are also used; these employ isotopes which do not fission thermally, like ^{238}U for which the fission reaction has a threshold at about 1 MeV. ^{238}U chambers are about 2-3000 times less sensitive than ^{235}U fission chambers with equal amount of fissile material. In both cases the count rate capability limit is C^{MAX} = 1 MHz (in pulse mode), while the minimum acceptable count rate is determined by the desired time resolution and statistical accuracy.

In ignited plasmas, the slowing-down time of fusion α-particles ($\tau_{s,\alpha} \approx 50$ ms in Ignitor) can be assumed as a typical time scale of variation of $Y_n(t)$. A time resolution $\Delta t \approx 100$ ms and a statistical accuracy $\sigma = \pm 13$ % or better, determine a minimum number of counts $N \approx 1000$ in Δt, hence determine a minimum count rate $C^{MIN} = 10$ kHz. This implies that the useful dynamic range is $D = C^{MAX} / C^{MIN} = 100$. The detector efficiencies ε (in units of cm^2) are defined as the ratio, $\varepsilon = C/F$, of the count rate over the neutron flux F at the detector location (in units of n/s cm^2), which vary proportionally with $Y_n(t)$. In order to cover a variation of five orders of magnitude in the neutron production rate, detectors of different efficiencies will be required.

The fluxes F have been calculated by MCNP [25] at various locations on the external surface of the cryostat. For example, the calculated neutron flux on the mid plane far from the horizontal ports is $F \approx 10^{-7} \times Y_n(t)$ cm^{-2} (only 10% of this flux consists of neutrons with energy > 1 MeV). Assuming $C^{MIN} = 10^4$ c/s for a minimum neutron production rate $Y_n(t) = 10^{15}$ n/s, a ^{235}U fission chamber in this position must have an efficiency $\varepsilon \geq 10^{-4}$ cm^2. On the other hand, a ^{235}U fission chamber with a lower efficiency must be employed at the same location to ensure a measurement up to the maximum neutron production rate $Y_n(t) \approx 10^{20}$ n/s. These efficiency values are standard for fission chambers. The dynamic range of fission chambers can be increased by several orders of magnitude considering also the current mode. However, the good discrimination against γ radiation is lost in passing from the pulse mode to the current mode [26].

It should be mentioned that non-fusion neutrons can be generated by photo-production caused by the interaction of runaway electrons with the wall. However, since this interaction is localised, photo neutrons can be discriminated against fusion neutrons employing several detectors at different toroidal angles around the device. On the other hand, the measurement of the photo neutron yield, provided by the neutron counters, can provide important information on the energy carried by the runaway electrons that is useful for evaluating the wall damage, especially during plasma disruptions.

Considering now the second aspect, the requirements on the accuracy in the absolute value of $Y_n(t)$ are very demanding, $\Delta Y_n/Y_n = 10$ % or better, and suggest the use of different and independent diagnostics [27].

Usually, absolute calibrations of neutron counters are obtained by employing neutron sources or generators with a well known intensity and situated in several toroidal and poloidal

locations inside the plasma chamber (in order to simulate the extended plasma source). This technique, called *in situ* calibration, has been routinely used in present devices operating with D plasmas, including FT and FTU [28]. The experience gained here suggests that many source locations are necessary to obtain an accurate calibration, since the streaming of neutrons through narrow penetrations, especially in compact devices, may give rise to non symmetric response functions of the detectors with respect to the toroidal location of the source. An example of response function to 2.5 MeV neutrons of one of the FTU fission chambers, is given in Fig. 3 and reference [25]. In Ignitor, the compactness of the device and the small port width (0.17 m), will limit the application of the *in situ* technique that, in this case, would require the use of a 14 MeV neutron tube. Here, neutron transport calculations may be usefully employed to study some problems encountered in the *in situ* calibration, such as the choice of the most suitable detector location, the experimental design and the integration of a limited set of experimental data.

The calibration of neutron counters remains however a difficult task. For example, D-T generators are typically much less intense than the plasma source (by a factor at least 10^{-7} in the Ignitor case), so that only the most sensitive detectors can be directly calibrated *in situ*; other detectors can only be cross calibrated varying the plasma neutron source in the appropriate ranges. In addition, changes in the machine auxiliary components near the tokamak may significantly change the detector response. Thus periodic recalibrations are necessary. For these reasons the Foil Activation Technique appears the most suitable mean to obtain an accurate absolute measurement of the (time integrated) neutron yield Y_n(t). This method has already been used in many tokamaks, both for 2.5 MeV and for 14 MeV neutrons (from triton burn-up), including FT, FTU and JET (see [29] , [30] and references therein). It requires the exposure of foils of suitable materials to the neutron flux close to the plasma chamber wall during a whole single discharge and the analysis of the induced radioactivity shortly afterward. For neutron yields from D-T plasmas, useful reactions must have threshold energies somewhat below 14 MeV, to reduce the contribution of scattered neutrons to the total activation. Since this contribution cannot be avoided but only reduced, the relationship between local fluence at the foil location and the emitted neutron yield must be calculated numerically. A recent benchmark experiment performed on FTU with 2.5 MeV neutrons [31], has shown that the activation technique can give an accurate measurement of Y_n(t) provided that the foils are exposed in a

simple casing as close as possible to the plasma, to minimise the contribution of collided neutrons to the total local fluence, and to simplify the numerical simulation. Moreover, the accuracy in modelling the real geometry of the scattering masses close to the foil irradiation position is decisive for the accuracy of the calculation. In order to obtain this, it is mandatory to integrate the Neutron Activation System (at least 4 irradiation ends at different poloidal angles through vertical tubes should be employed to correct for plasma displacement effects) in the Ignitor design from its initial phases.

Activation measurements at 14 MeV will be very useful also in the D operation phase, to verify the single particle behaviour of α's in Ignitor plasmas, through triton burn-up studies. These studies have been successfully performed in a number of devices operating in deuterium, including FT [32] and JET [33].

Another important application of the activation technique is the determination of the neutron energy spectrum at the irradiation position, close to the first wall. This can be obtained making use of materials and reactions with different energy thresholds. This information would be useful for checking the evaluations of radiation damage and the activation of the structures close to the plasma.

Finally, the total neutron yield can be determined by integration of the neutron camera measurements (see below). The accuracy is limited by the absolute calibration of the detectors and by geometrical factors [34].

Neutron Emissivity Profile Measurements

Ignitor will produce intense collimated neutron fluxes. As a consequence, collimated neutron measurements (time and space differential) may be expected to gain in importance. This calls for neutron detectors of high performance, with regard to count rate capability (> 1 MHz), calibration accuracy (≈ 1%) and energy resolution, to form the basis for new designs of neutron spectrometers and collimator arrays [35, 36, 37, 38].

The neutron emissivity in thermonuclear plasmas is related to the ion temperature and density through the relation $S(r,\vartheta) = n_T\, n_D\, \langle\sigma v\rangle$, where the maxwellian reactivity $\langle\sigma v\rangle$ is a function of the ion temperature and can be approximated for simplicity as $\langle\sigma v\rangle \approx T^{\gamma}$. For example, for the D-T maxwellian reactivity, $\gamma \approx 5$ for $1 < T < 5$ keV and $\gamma \approx 3$ for $5 < T < 15$

keV. If the ion temperature and density can be modelled as: $n_T = n_D = n_o (1-\rho^2)^{\alpha_n}$, $T = T_o (1-\rho^2)^{\alpha_T}$ where $\rho = r/r_p(\vartheta)$ and $r_p(\vartheta)$ describes the plasma D-shaped edge, then the neutron emissivity can be modelled as $S(\rho) = S_o (1-\rho^2)^{\alpha}$ where $\alpha = 2\,\alpha_n + \gamma\alpha_T$ and $S_o = n_D(0)\, n_T(0)\, \langle\sigma v\rangle_{T=To}$ is the emissivity on the axis.

The measurement of the spatial distribution of the neutron emission employs arrays of collimators and detectors (neutron cameras) that receive the neutron emission from well defined chordal volumes of the plasma in one plane, usually the poloidal plane. The number of channels must be such as to view most of the emitting plasma, extending symmetrically from the centre of the plasma outwards as far as there is sufficient neutron intensity to be measured; the practical limit is $\approx 10^2$ the central peak intensity. Every single collimator defines a line of sight, or a chord through the plasma, as sketched in Fig. 4; collimated measurements should aim at a spatial resolution $\Delta x < a/10$, where a is the plasma minor radius. Usually, $\Delta x \approx 5 \div 10$ cm must be maintained in order not to sacrifice the count rate and the time resolution, especially in a plasma region where the local emissivity is low. When two orthogonal cameras (vertical and horizontal) are available, a tomographic reconstruction of the emissivity profile is possible. In Ignitor it will be possible to implement only a horizontal camera, viewing the plasma through one of the horizontal ports; hence only the line integrated emissivity could be obtained and the complete reconstruction of the emissivity profile must rely upon the knowledge of the shape of the magnetic flux surfaces from magnetic measurements and equilibrium calculations. These measurements are usually less accurate in the plasma centre where most of the neutrons are emitted. Therefore the presence of at least one vertical channel would be very useful for obtaining the elongation of the hot plasma core.

Under thermal plasma conditions, the first information derived from the camera measurements is the product $n_T \times n_D$ (line averaged, or local values if profile reconstruction is possible) when the ion temperature profile T_i is known independently from spectroscopic measurements. The other important piece of information is the a particle birth profile [39] which, for the plasma currents typical of Ignitor discharges, should be very close to the α-particle heating deposition unless significant radial diffusion occurs. These pieces of information are fundamental to understanding the physics of burning plasma.

As a preliminary design, a set of horizontal collimators is considered with a length L = 4.6 m and a circular cross section of area A_c = 10 cm^2 (see Fig. 4 and references [24]-[37]). The detectors may be located behind the bunker wall, which can be used as part of the shield. The detector distance from the plasma centre in this case is D = 7.5 m. Given the Ignitor port size, it is possible to employ a fan type collimator with 9 channels, covering 65% of the whole plasma. The FWHM of the viewed plasma volume Δx is approximately Δx = 6.5 cm. Given the collimation geometry, the number of neutrons Y_i generated in the volume seen by i-th channel can be calculated for particular values of the peaking factor α of the neutron emissivity [24]. The fluxes at the detectors are then given by $F_i = Y_i / 4\pi^2$ (n/cm^2s). For the chosen collimator geometry, F_i varies from around $10^{-10}\ Y_n$ in the central channel to $10^{-11}\ Y_n \div Y_n\ 10^{-13}$ in the peripheral channel for $\alpha = 4 \div 14$. These numbers can be used to determine the detector characteristics. Given the large variation of Y_n during the initial transient phase of the discharge, the range of operation of the multicollimator could be fixed to start with T > 4 keV, hence in the range $10^{18} < Y_n < 10^{20}$ n/s. A detector in the central channel, with a sensible area equal to the channel cross section, having an efficiency $\varepsilon = 10^3$ cm^2 will have $C \approx 10^{-10} \div 10^{-4} \times Y_n$ counts/s, that is $C \approx 10^5 \div 10^7$ counts/s in the range of interest. The flux in the most external channel can vary from 10^{-1} to 10^3 times the flux in the central one, depending on the profile. For this channel the additional factor > 100 in the profile changes should be added to the given 10^2 variation in the neutron production rate, hence the corresponding detector should have a dynamic range of at least 10^4. For example, a detector with $\varepsilon = 10^{-3}$ cm^2, will have $C \approx 10^2 \div 10^6$ counts/s in the ranges of interest of Y_n and α.

The shielding material and configuration for collimated (and spectral) neutron measurements require a careful analysis. In fact, the experience made in present tokamaks with 2.5 MeV neutrons has shown the presence of high levels of gamma radiation with energy of several MeV, mostly generated by neutron capture in the shielding materials surrounding the detectors. The problem is not expected to ameliorate in passing from 2.5 to 14 MeV neutrons. The captured gamma radiation can be strongly reduced by an appropriate choice of shielding material; suitable detectors to be used in the multicollimator should however be intrinsically insensitive to gamma radiation.

The detectors should also have sufficient energy resolution to discriminate against background neutrons back scattered from the inner first wall that will inevitably contaminate the measurement to a non negligible amount [24]. Examples of neutron spectra in the central channel and in a peripheral channel are given in Fig. 5.

The use of Magnetic Proton Recoil detectors (MPR) as counters in the camera meets all requirements for measurements of D-T neutrons [33]. The MPR technique (described in the next section) is free of gamma contamination and should provide passively the required energy discrimination. For the camera counters, an energy resolution $\delta E_R/E = 15\%$ is needed in order to discriminate against scattered, energy degraded neutrons, especially in the peripheral channels. An efficiency up to 10^{-3} cm^2 can be achieved, as required.

Neutron Spectrometry Measurements

The basic plasma information that can be obtained in spectrometric measurements, especially in burning D-T plasmas at ignition but also in D-T plasmas at lower fusion power and in D-D plasmas, are:

1) the ion temperature T_i ;
2) the fuel density product $n_D \times n_T$;
3) the fusion spectrum composition in terms of thermal and supra-thermal components.

Below, a neutron spectrometer system is described, that is designed to provide this information over a broad range of Ignitor plasma conditions.

During the ignition phase, the spectrometer must operate at high count rate [40] to afford sufficient time resolution; it should also have an energy resolution (δE_R) matching the ion temperature of these plasmas, $\delta E_R/E = 2.5$ % corresponding to $T_i = 4$ keV or higher [38]. The experiments devoted to burn condition formation will involve numerous discharges of lower temperatures and neutron yields and this will require spectrometers of better resolution ($\delta E_R/E=1.8\%$, corresponding to $T_i = 2$ keV) and also high efficiency. Moreover, it can be anticipated that neutron spectrometry measurements of 2.5 MeV neutrons from D-D reactions will be desirable because much of the operation would be with D-D plasmas including those with very small amounts of tritium seeding. This would call for spectrometers with very high

efficiency to maintain high count rate at rather low neutron fluxes; the resolution should be $\delta E_R/E = 4.8$ %, corresponding to $T_i = 2$ keV.

The choice of detection methods for 14 MeV neutrons with energy resolution is rather limited. The Magnetic Proton Recoil spectrometer (MPR) has been preferred for Ignitor because of its ability to handle high count rates and is the only method that can make full use of the high fluxes expected from Ignitor [41]. It would ensure data of the highest possible quality during the plasma burn period of the discharge, relying on count rates in the range 0.1 to 1 MHz and being able to cope with any overshoots into the $1 \div 100$ MHz range.

The MPR consists of a magnetic spectrograph viewing the recoil protons produced by the neutron beam impinging on a thin CH_2 foil. The protons are focused, deflected and momentum analysed in a magnet system and detected in a proton counter array at the spectrometer exit [42]. The incoming neutron energy is recorded in a histogram as a function of counter number. Specifications of the MPR spectrometer are given in Table 1.

The design and construction of a prototype MPR spectrometer are in progress [43]. See [44] for a detailed description of an earlier version of the instrument based on a quadrupole-dipole-quadrupole (QDQ) magnet system.

For D-D neutrons high detection efficiency and corresponding count rate capability are the main priority. This can be achieved with the Time of Flight (TOF) technique. This is used for measuring neutron spectra in nuclear physics experiments where the neutron TOF can be determined relative to the time structure of a pulsed beam. For fusion neutrons, dual timing signals must be used. The first comes from a scintillation detector in the neutron beam (S_1) where the $n+p_H \rightarrow n'+p$ scatterings are manifested through the proton recoil signal. The second signal comes from another scintillator (S_2) for the scattered neutron having travelled a known flight path distance.

A TOF spectrometer of the in-beam geometry has been used at JET [44]. The documented JET experience suggests that the count rate capability C_n^{CAP} is one of the principal handicaps [38]. The intrinsic upper count limit of a TOF spectrometer is $C_n^{CAP} = 5$ MHz in a pure neutron beam (in the case of 2.5 MeV neutrons from thermal D+D reactions). This is a theoretical limit which is approached in proportion to a value of the catching factor $\chi \rightarrow 1$ (the catching factor is defined as the fraction of the selected events in S_1 that is also recorded in S_2).

The JET spectrometer has $\chi < 10^{-3}$ and has $C_n^{CAP} \approx 10$ kHz. The usefulness of the TOF spectrometer for Ignitor depends crucially on being able to boost the catching factor some two orders of magnitude to $\chi \geq 0.05$. This is considered feasible as shown in ref. [45]. It is expected to reach $\chi = 0.07$ giving $C_n^{CAP} = 350$ kHz. This requires a special design where the S_2 scintillator is shaped to follow the curved surface on the constant TOF sphere. The specification of the TOF_p spectrometer proposed for the Ignitor measurements are given in Table 2.

The studies of ignition plasma formation in Ignitor would entail lower neutron flux so that high detection efficiency ($\varepsilon = 10^3$ cm^2) is a priority property for a complement to MPR. This can also be provided by the TOF method. For 14 MeV neutrons it is best to use a deuterated in-beam scintillator relying on $n+D_T \rightarrow n'+D$ scattering reaction in the back angle scattering geometry. The TOF_d spectrometer has been described earlier in a design for JET [46] and here the design should be adapted for operation with a narrowly collimated neutron beam (area $A_c = 10$ cm^2) so that it could share the beam line with MPR [38]. The TOF spectrometer can be operated with different combinations of resolution and efficiency. For Ignitor one could mainly consider operation in a high resolution mode. The corresponding specifications are given in Table 3.

A suitable location for the MPR + TOF_D + TOF_p spectrometer system envisaged for Ignitor would be outside the bunker wall, at a distance of about 7 m from the plasma. A collimator (aperture $A_c = 10$ cm^2 and length about $L_c = 2$ m) would provide an effective plasma viewing area of $A_p = 100$ cm^2 through a diagnostic port of the machine (Fig. 6).

This would represent an adequate spatial resolution in the transverse direction and it would also satisfy the desire for high neutron fluxes ($F_n^{MAX} = 2 \times 10^{10}$ n/scm^2 for the fusion yield at ignition $Y_n^{MAX} = 3 \times 10^{19}$ n/s) in order to exploit the count rate capability of the MPR spectrometer. All spectrometers can be located at the same port and collimation aperture. The remote location combined with the large information output (they provide information on both temperature and density) makes them quite acceptable for use in Ignitor on space economy grounds. Moreover, the neutron spectrometers suggested should be able to operate well within the experimental conditions around Ignitor. Although Ignitor may produce high radiation fluxes,

the fluences should be rather limited by the short pulse lengths to be used. Therefore the use of in-beam scintillators should be acceptable.

Although the MPR technique is most effective for 14 MeV neutrons, it could be used also for 2.5 MeV neutrons. A tandem MPR spectrometer system [47] could simultaneously measure the 2.5 MeV neutron minority flux (from d+d reactions in D-T plasmas) and the 14 MeV flux. Similarly, the MPR counter in the camera could be modified for use in the D-D phase operation which is especially attractive for determining Y_n of D and D-T plasmas on the same footing.

6. Layout of Planned Diagnostic Systems and Required Access

We consider the set of the 13 diagnostics systems summarised in the following to be adequate to provide the information necessary to characterise the physical regimes that Ignitor can produce [14]. Only a part of the system is hardened against the high flux of 2.5 MeV and 14 MeV neutrons, γ and X-rays. During the operation further or better hardening may in fact be needed.

The present proposal is largely inspired by the studies made for the FTU machine by the ENEA Plasma Physics Division. The required access is 12 T-shaped sectors, each having two vertical and one horizontal windows. The oval vertical windows should be centered at three different radial positions, looking at the plasma from 5 cm to 20 outward; the horizontal windows extend 40 cm above and below the torus midplane (see Fig. 7). Six horizontal ports are allocated to the RF antennae and are not available for diagnostic purposes. This represents a total of 12×2+6=30 ports (FTU has 24 ports for diagnostics and JET 36). The distribution of the diagnostics around the machine is, at the present time, preliminary. A more definite plan will be possible when the real size and the space requirements for the individual diagnostics are known and when the allocated spaces outside the biological wall are determined.

Diagnostic System 1 - Electrical Measurements

- Measured parameters:
    - voltage and current of the plasma loop;
    - plasma pressure;

- magnetic flux surfaces, shape and position;
- MHD activity.

Diagnostic System 2 - Soft X-ray Intensity

- Measured parameters:
  - sawteeth;
  - MHD activity;
  - ΔZ_{eff}, ΔT_e.
- Sensors:
  - arrays of Si (Li) diodes with relative pinhole optics put near the vertical and horizontal windows: 20+20 for 1 sector;
  - memory requirements: 40×3 kbyte/pulse = 120 kbyte/pulse.
- Not hardened.

Diagnostic System 3 - Soft X-ray Spectrometry

- Measured parameters:
  - ion temperature;
  - electron temperature;
  - impurity concentration.
- Device:

  A curved crystal spectrometer in the Johann configuration, with high spectral resolution ($\lambda / \Delta\lambda \cong 10000$), possibly equipped with multiple crystals for spatial profiles and a single 2-D Multiwire Proportional Counter detector. The Bragg angle should be $60^o > \theta_B > 50^o$, and the distance of the crystal to the plasma, and the crystal to the detector can be anywhere from 5 to 20 m, possibly around 12 m. The crystal(s) can be placed outside the biological wall, with the rest of the output arm and detector. In this case additional screening is required, similar to the spectrometer built under contract by ENEA-Frascati at JET. This diagnostic can be made radiation hard.

Diagnostic System 4 - Bolometry

- Measured parameters:
    - radiated power;
    - radial emissivity profile.
- Sensors:
    - an array of 36 metal-resistor bolometers;
    - the bolometers will be in direct view of the plasma on a horizontal port.
- Hardened.

Diagnostic System 5 - Spectrometry (visible to VUV)

- Measured parameters:
    - recycling;
    - $Z_{eff}(r,t)$;
    - $n_z(r,t)$ impurities.
- Sensors:
    - D_α array to study the recycling, UV (200 - 3000 Å) and VUV (15-1100 Å) spectrometers in direct view of the plasma;
    - the detectors will stay inside the biological wall.
- Limited hardening can be provided by in situ local screening.
- Additional proposal: VUV Spatial Scan Spectrometry.
- Measured parameters:
    - impurity content.
- Brief description: the system is composed of 2 rotating mirrors and 2 spectrometers connected with photo multipliers.

Diagnostic System 6 - Thomson Scattering

- Measured parameters:

- T_e (r,t) at ten different times;
- n_e (r,t) at ten different times.

- Apparatus:
  - the light impulse is produced by a neodymium Q-switched laser of an energy > 7 Joules that is able to produce ten flashes at various time intervals during the plasma discharge;
  - the laser and the polychromator are outside the biological wall. The scattered light is piped out by special fiber optics;
  - several polychromators are foreseen for the different temperature ranges;
  - the plasma is measured at ten different radii. The output is given by a matrix of 10×10 diodes.

Diagnostic System 7 - Electron Cyclotron Emission

- Measured parameters:
  - T_e (r,t);
  - supra thermal electrons.
- Apparatus:
  - the wave guides pick up the ω_{CE} emission near the plasma;
  - the EM radiation is then piped outside the biological wall into the interferometers (Michelson, Fabry-Perot and detected);
  - time resolution < 10 ms.
- Hardened.

Diagnostic System 8 -Two Colour CO_2 Interferometer

- Measured parameters:
  - n_e (r,t)
- Apparatus:
  - the CO_2 laser beam (200 W) beam (λ = 10.6 μm) is widened and sent through a vertical window across the plasma. Part of it is deflected towards the horizontal port, where retroflectors are located; the light is sent back and

collected by the detection optics. Four or five line of sights can be obtained, more if another port, at a different toroidal and radial location is also used;

- the effects of vibrations are minimised by using a second laser of a different colour (λ = 3.39 μm) sharing the same optical path;
- the laser and the detectors are situated outside the biological wall.

- Hardened.

Diagnostic Systems 9 - 10 -11 - Neutron Measurements

- Measured parameters:
  - absolute neutron yield in a shot;
  - radial distribution of the neutron emissivity;
  - neutron energy distribution;
  - ion temperature and/or ion density.
- Brief description:
  - fission chambers and foil activation system;
  - high resolution neutron spectrometers;
  - multicollimator array.

Diagnostic System 12 - Charged Particle Diagnostic

- Measured parameter:
  - spectrum of the charged particles escaping from the plasma.

- Brief description:
  - the system is composed of a plastic scintillator, mounted inside the plasma chamber, connected by a fiber optic system to a P.M.
- Some information on the particles escaping from plasma (triton in a deuterium plasma) can be obtained by activation analysis.

Diagnostic System 13 - Hard X-ray Measurements

- Measured parameter:
  - bremsstrahlung radiation produced by runaway electrons.

- Brief description:
    - the system consists of two groups of four Sodium Iodide scintillators coupled to photo multipliers.

$\varepsilon = 7\times10^{-3}$ cm^2	detector efficiency
$\delta E_R/E \leq 2.5\%^*$	energy resolution
$C_n^{CAP} = 25 - 100$ MHz**	count rate capability
$F_n^{MAX} = 1\text{-}5\times10^{12}$ n/scm^2	maximum neutron flux

Table 1 Parameter for MPR spectrometer for 14 MeV neutrons.

* This corresponds to Doppler broadening of d+t-ions at T_i=3.9 keV.

** Depending on width of neutron spectrum.

$\varepsilon = 1\times10^{-2}$ cm^2	detector efficiency
$\delta E_R/E \leq 5\%^*$	energy resolution
$C_n^{CAP} = 350$ kHz	count rate capability
$F_n^{MAX} = 3.5\times10^7$ n/scm^2	maximum neutron flux
$\chi = 0.07$	catching factor

Table 2 Parameter for TOF_p spectrometer for 2.5 MeV neutrons.

* Corresponds to Doppler broaderning of D-ions at T_i=2.2 keV.

$\varepsilon = 7\times10^{-4}$ cm^2	detector efficiency
$\delta E_R/E \leq 1.8\%^*$	energy resolution
$C_n^{CAP} = 80$ kHz	count rate capability
$F_n^{MAX} = 1\times10^8$ n/scm^2	maximum neutron flux
$\chi = 0.03$	catching factor

Table 3 Parameter for TOF_d spectrometer for 14 MeV neutrons.

* Corresponds to Doppler broadening of D+T-ions at T_i=2 keV.

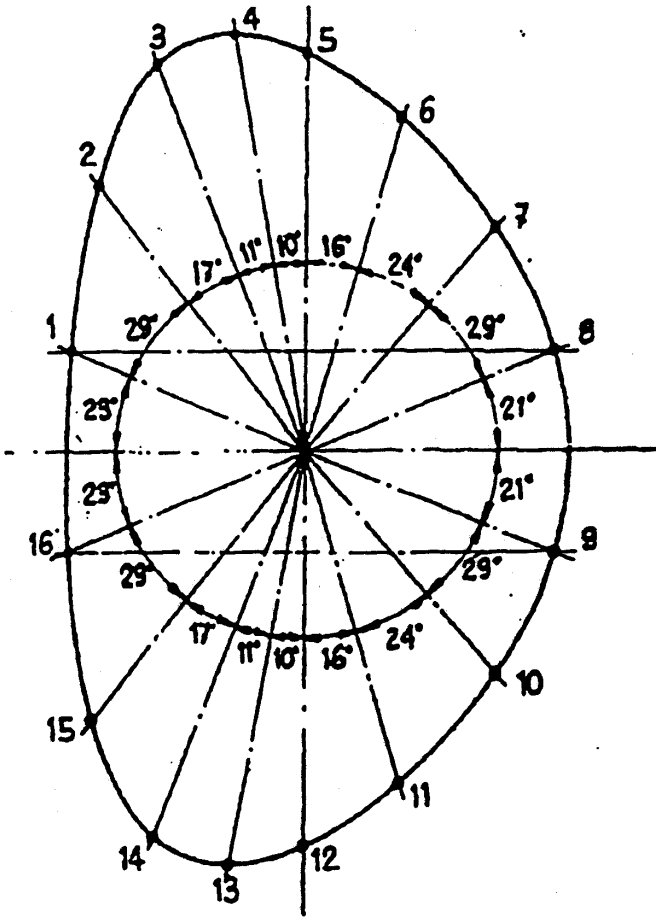

Figure 1 Poloidal distribution of the magnetic coils.

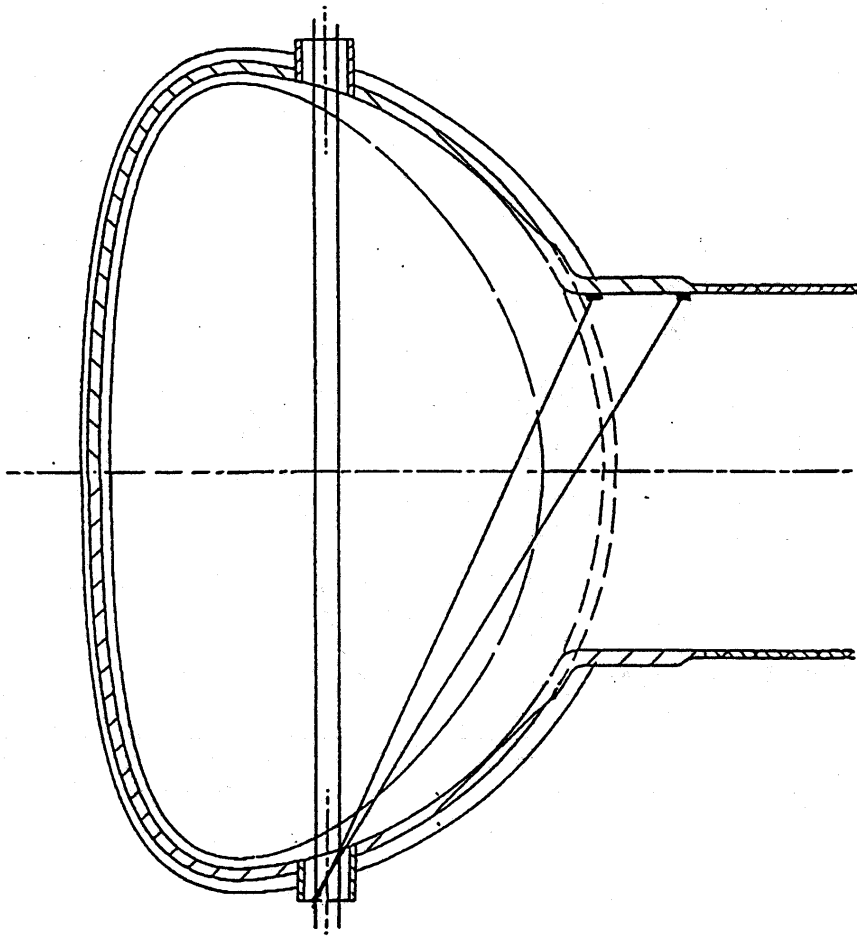

Figure 2 Tentative chords for the CO_2 interferometer.

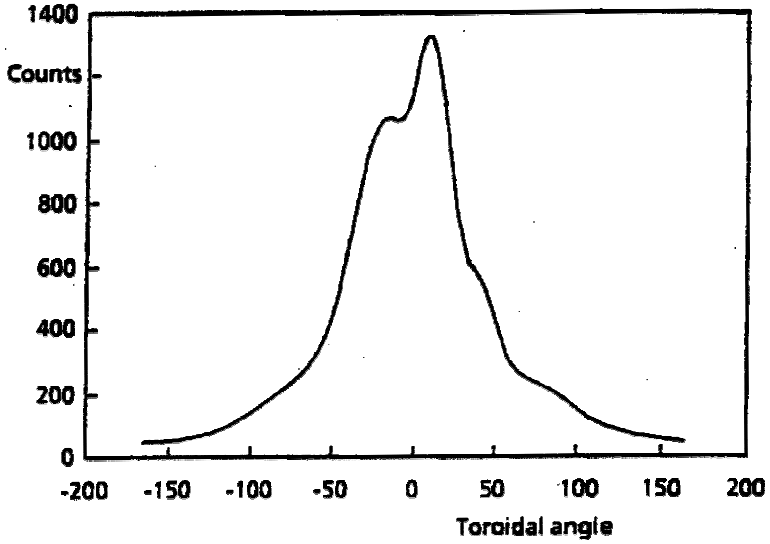

Figure 3 Geometrical efficiency of one of the FTU fission chambers (^{235}U), obtained in the 1989 calibration, as a function of the location of the ^{252}Cf source in the torus. The fission chamber is located outside the FTU cryostat. The non-symmetric response of the detectors with respect to the toroidal location of the source is clearly evident.

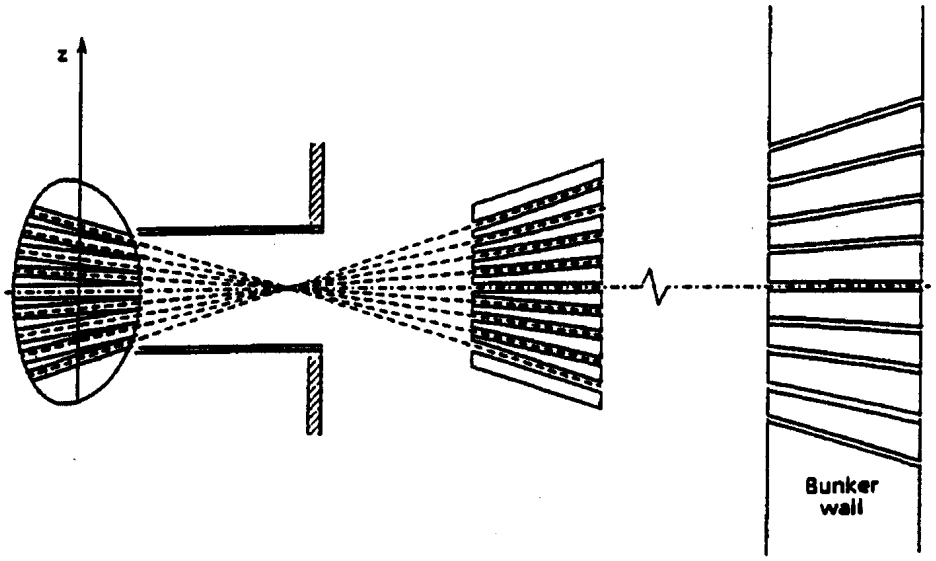

Figure 4 Meridian cross section of the plasma, horizontal port and layout of the multichannel collimator.

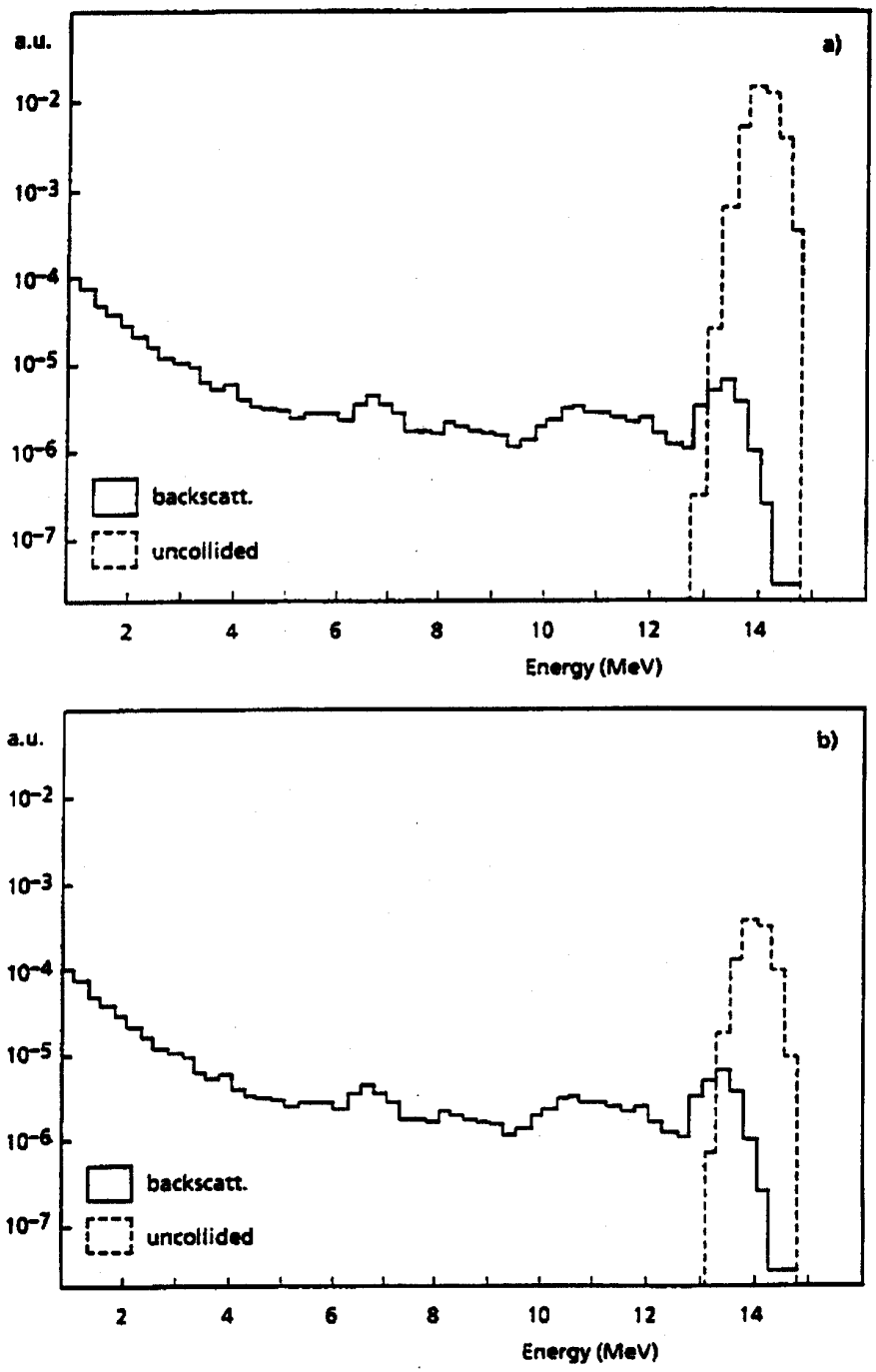

Figure 5 Calculated energy spectra of neutrons impinging (a) in the central and (b) in the peripheral channel of the Ignitor multicollimator. The hatched line represents the uncollided flux from the plasma source with T=10 keV, while the solid line represent the flux backscattered from the inboard first wall.

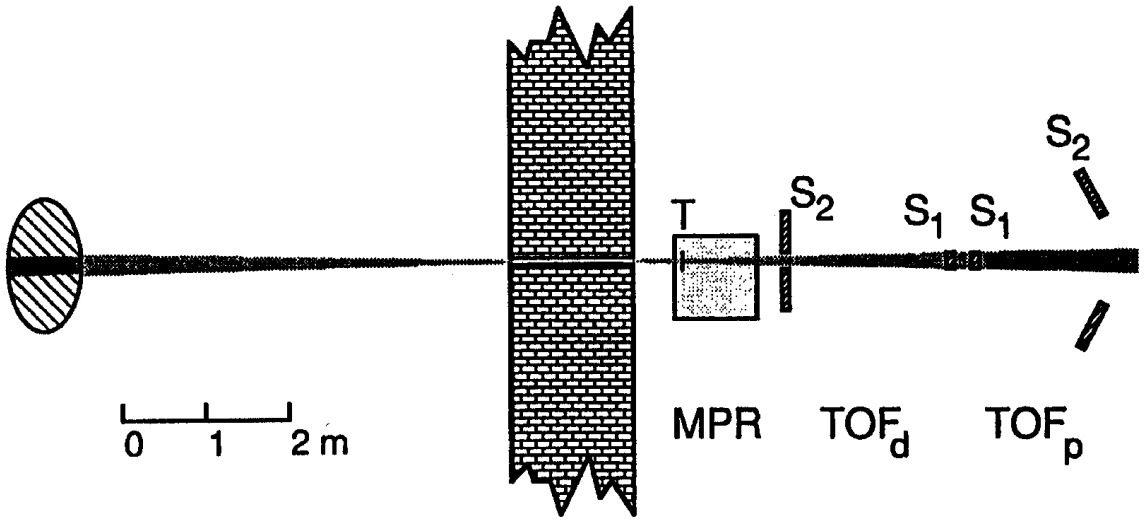

Figure 6 Poloidal cross section of the plasma, the bunker wall and layout of the MPR+TOF_D+TOF_p spectrometer system.

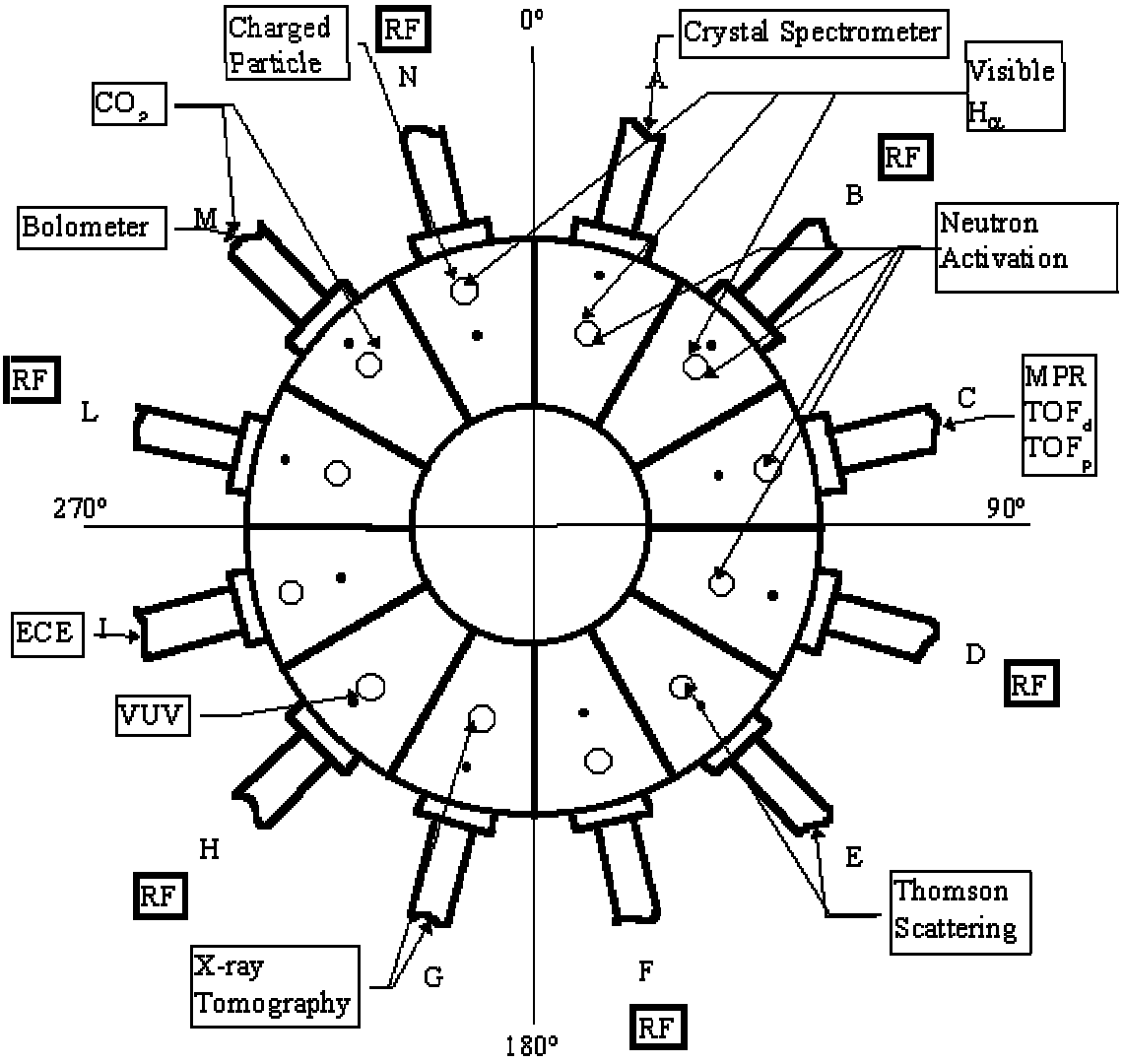

Figure 7 Required access for the diagnostics. The actual distribution of the ports allocated to diagnostics will have to take into account that 6 ports will be devoted to the ICRF antennae.

References

[1] The Ignitor Program Group, "Ignitor Project Feasibility Study," status report November 27, 1988, published by E.N.E.A., Viale Regina Margherita 125, Rome, Italy (1989).

[2] M. Bornatici, R. Cano, O. De Barbieri and F. Engelmann, *Nucl. Fusion* **23**, 1153 (1983).

[3] P. Buratti, O. Tudisco and M. Zerbini, *Infrared Phys.* **34**, 533 (1993).

[4] P. Buratti, O. Tudisco and M. Zerbini, in ISPP-9 «Piero Caldirola», "Diagnostics for Contemporary Fusion Experiments", SIF, Bologna 1991, p. 787.

[5] P. Buratti and M. Zerbini, *Rev. Sci. Instrum.* **66**, 4208 (1995).

[6] P. Buratti and M. Zerbini, Proc. of the *EC-9 Workshop* (Borrego Springs, 23-26 January 1995), World Scientific, Singapore 1995, p. 409.

[7] D. Johnson et al., *Rev. Sci. Instrum.* **56**, 1015 (1985).

[8] E. Hinnov et al., *Nucl. Instr. Meth.* **202**, 381 (1982) and J.L. Schwob et al., *Rev. Sci. Instr.*, **58**, 1601 (1987).

[9] R. Bartiromo et al., *Rev. Sci. Instr*. **60**, 237 (1988).

[10] K.F. Mast et al., *Rev. Sci. Instr.* **56**, 908 (1985).

[11] M. Bitter et al., *Phys. Rev. Lett.*, **71**, 1007 (1993).

[12] R. Bartiromo et al., in *Course on Diagnostics for Contemporary Fusion Experiments*, Varenna, Italy, 1991, p. 959.

[13] F. Bombarda et al., *Nucl. Instr. Meth.* **222**, 563 (1984).

[14] M. Mattioli et al., *J. Appl. Phys*. **64**, 3345 (1988).

[15] P. Innocente, S. Martini, *Rev. Sci. Instrum.* **63**, 4996 (1992).

[16] J.H.Irby, E.S. Marmar, E. Sevillano, S.M. Wolfe, *Rev. Sci. Instrum.* **59**, 1568 (1988).

[17] F.C. Jobes and D.K. Mansfield, *Rev. Sci. Instr*. **63**, 5154 (1992).

[18] R.Wunderlich, W.Schneiderand, K.Lackner, "Entfaltungwon Bolometer-signalen am Tokamak ASDEX Upgrade", IPP 5/37 (Jan. 1992).

[19] R.S.Granetz, P.Smeulders, "X-Ray Tomography on JET", *Nuclear Fusion* **28**, 457 (1988).

[20] M.H.Van de Voorde and C.Restat, CERN Report 72-7, Geneva, (1972).

[21] J.F.Kirchner and R.E.Bowman, "Effects of Radiation on Mat. and Compon.", Reinhold Publ.Corpor. New York.

[22] E. Bittoni, M. Haegi, *Fusion Technology* **22**, 461 (1992).

[23] E. Mazzucato, "Study of α-Heating,", *Ignitor Workshop*, July 1992, Turin, Italy.

[24] S. Rollet, P. Batistoni, *Rev. Sci. Instrum.* **63**, 4551 (1992), or in a more extended version: P. Batistoni, S. Rollet, "Neutron transport studies for the Ignitor Neutron Diagnostics", ENEA Report RT/NUCL/91/30 (1992).

[25] "MCNP: A General Purpose Monte Carlo Code for Neutron and Photon Transport", LA-7396-M (Revised Version 3A), Los Alamos National Laboratory, Sep. 1986.

[26] O. N. Jarvis, "Neutron Detection Techniques for Plasma Diagnostics", *Course on Diagnostics for Fusion Reactor Conditions*, International School on Plasma Physics, Varenna, September 6-17 1982, EUR 8351-I EN , Vol. 1, p.353.

[27] J. D. Strachan, J. M. Adams, C. W. Barnes, P. Batistoni, H. S. Bosch et al., *Rev. Sci. Instrum*. **61**, 3501 (1990).

[28] M. Angelone, P. Batistoni, L. Bertalot, B. Esposito, M. Martone, M. Pillon, S. Podda, M. Rapisarda, S. Rollet, *Rev. Sci. Instrum*. **61**, 3536 (1990).

[29] M. Angelone, P. Batistoni, L. Bertalot, B. Esposito, M. Martone et al, *Rev. Sci. Instrum*. **61**, 3157 (1990).

[30] O.N. Jarvis, E.W. Clipsham, M. A. Hone, B. J. Laundy, M. Pillon, et al. *Fusion Technology* **20**, 265 (1991).

[31] M. Angelone, P. Batistoni, M. Martone, M. Pillon, M. Rapisarda, S. Rollet, *Fusion Technology* **19**, 431 (1991).

[32] P. Batistoni, M. Martone, M. Pillon, S. Podda, M. Rapisarda, *Nuclear Fusion* **27**, 1040 (1987).

[33] J. Källne, P. Batistoni, G. Gorini, G. B. Huxtable, M. Pillon et al., *Nuclear Fusion* **28**, 1291 (1988).

[34] M. Martone, P. Batistoni, L. Bertalot, M. Pillon, S. Podda, "Analysis and preliminary Design of Neutron Diagnostics for NET", NET Rep.EUR-FU/XII-80/88-86.

[35] J. Källne, *Comm. Plasma Phys. Contr. Fusion* **12**, 235 (1989), and J. Källne, "Neutron measurements in the study of fusion plasma physics with tokamaks", Rep. PTP 88/11, MIT, Cambridge Massachusetts (1988).

[36] G. Gorini , J. Källne, S. Rollet, *Proc. 17th Conf. Controlled Fusion and Plasma Heating*, Amsterdam 1990, **14B**, Part IV, 1652.

[37] J. Källne, P. Batistoni, B. Coppi, R. Dierckx, G. Gorini, M. Martone, L.Perasso, S. Rollet, *Proc. 7th ASTM-Euratom Symposium on Reactor Dosimetry*, Strasbourg 27-31 August , 1990, p. 429.

[38] G. Gorini,J. Källne, *Il Nuovo Cimento* **14D**, 1115 (1992).

[39] J. Källne, G. Gorini, *Fusion Technology* **22**, 439 (1992).

[40] G. Gorini, J. Källne, *Com. Plasma Phys. Contr. Fusion* **15**, 193(1993).

[41] J. Källne, G. Gorini, *Rev. Sci. Instrum*. **64**, 2765 (1993).

[42] J. Källne, G. Gorini, *Proc. Course and Workshop*, Varenna,1991 Vol. ISPP-9,1033.

[43] J. Källne, G. Gorini, H. Cond, P. U. Renberg, *Proc. Int. Conf. on Plasma. Physics*, Innsbruck, 1992, vol. 16c, Part II, 1047.

[44] J. Källne, Uppsala University Neutron Physics Report UU-NF 01/91, Uppsala(1991) and NET Physics Memo PM90-003, Garching, (1991); J. Källne, H.Enge, *Nucl. Instr. Methods* **A311**, 595 (1992).

[45] G. Gorini, J. Källne, *Rev. Sci. Instrum.* **63**, 4548 (1992).

[46] J. Källne, G. Gorini, O. N. Jarvis, G. Martin, V. Merlo, G Sadler, P. van Belle, *Physica Scripta* **T16**, 160 (1987); J. Källne, T. Elevant, "Neutron Time of Flight Spectrometer for Diagnostics of D-T Fusion Plasma", Rep. JET-P (85) 03, JET Joint Undertaking, Abingdon, (1985).

[47] J. Källne, P. Batistoni, G. Gorini, *Rev. Sci. Instrum*. **62**, 2871 (1991).